Bifractal focusing and imaging properties of Thue–Morse Zone Plates

Vicente Ferrando,[1,2] **Fernando Giménez,**[3] **Walter D. Furlan,**[2] **and Juan A. Monsoriu**[1,*]

[1]*Centro de Tecnologías Físicas, Universitat Politècnica de València, E-46022 Valencia, Spain*
[2]*Departamento de Óptica, Universitat de València, E-46100 Burjassot, Spain*
[3]*I.U. Matemática Pura y Aplicada, Universitat Politècnica de València, E-46022 Valencia, Spain*

[*]*jmonsori@fis.upv.es*

Abstract: We present a new family of Zone Plates (ZPs) designed using the Thue-Morse sequence. The focusing and imaging properties of these aperiodic diffractive lenses coined Thue-Morse Zone Plates (TMZPs) are examined. It is demonstrated that TMZPs produce a pair of self-similar and equally intense foci along the optical axis. As a consequence of this property, under broadband illumination, a TMZP produces two foci with an extended depth of focus and a strong reduction of the chromatic aberration compared with conventional periodic ZPs. This distinctive optical characteristic is experimentally confirmed.

OCIS codes: (050.1940) Diffraction; (050.1965) Diffractive lenses; (050.1970) Diffractive optics.

References and links

1. J. Ojeda-Castañeda and C. Gómez-Reino, *Selected Papers on Zone Plates* (SPIE Optical Engineering Press, 1996), vol. MS128.
2. Y. Wang, W. Yun, and C. Jacobsen, "Achromatic Fresnel optics for wideband extreme-ultraviolet and X-ray imaging," Nature **424**, 50–53 (2003).
3. S. Wang, X. C. Zhang, M. P. Maley, M. F. Hundley, L. N. Bulaevskii, A. E. Koshelev, and A. J. Taylor, "Terahertz tomographic imaging with a Fresnel lens," Opt. Photonics News **13**, 58 (2002).
4. E. Maciá, "The role of aperiodic order in science and technology," Rep. Prog. Phys. **69**, 397–441 (2006).
5. G. Saavedra, W. D. Furlan, and J. A. Monsoriu, "Fractal zone plates," Opt. Lett. **28**, 971–973 (2003).
6. J. A. Monsoriu, A. Calatayud, L. Remón, W. D. Furlan, G. Saavedra, and P. Andrés, "Bifocal Fibonacci diffractive lenses," IEEE Photonics J. **5**, 3400106 (2013).
7. W. D. Furlan, G. Saavedra, and J. A. Monsoriu, "White-light imaging with fractal zone plates," Opt. Lett. **32**, 2109–2111 (2007).
8. X. Ge, Z. Wang, K. Gao, D. Wang, Z. Wu, J. Chen, K. Zhang, Y. Hong, P. Zhu, and Z. Wu, "Effects of the condenser fractal zone plate in a transmission X-ray microscope," Radiat. Phys. Chem. **95**, 424–427 (2014).
9. S. H. Tao, B. C. Yang, H. Xia, and W. X. Yu, "Tailorable three-dimensional distribution of laser foci based on customized fractal zone plates," Laser Phys. Lett. **10**, 035003 (2013).
10. Q. Zhang, J. Wang, M. Wang, J. Bu, S. Zhu, B. Z. Gao, and X. Yuan, "Depth of focus enhancement of a modified imaging quasi-fractal zone plate," Opt. Laser Technol. **44**, 2140–2144 (2012).
11. Q. Q. Zhang, J. G. Wang, M. W. Wang, J. Bu, S. W. Zhu, R. Wang, B. Z. Gao, and X.-C. Yuan, "A modified fractal zone plate with extended depth of focus in spectral domain optical coherence tomography," J. Opt. **13**, 055301 (2011).
12. Y. J. Liu, H. T. Dai, X. W. Sun, and T. J. Huang, "Electrically switchable phase-type fractal zone plates and fractal photon sieves," Opt. Express **17**, 12418 (2009).
13. Y. Fu, W. Zhou, and L. Lim, "Propagation properties of plasmonic micro-zone plates with and without fractals," Appl. Phys. B **90**, 421–425 (2008).

#242496 Received 8 Jun 2015; revised 13 Jul 2015; accepted 16 Jul 2015; published 22 Jul 2015

14. V. Ferrando, A. Calatayud, P. Andrés, R. Torroba, W. D. Furlan, and J. A. Monsoriu, "Imaging properties of kinoform Fibonacci lenses," IEEE Photonics J. **6**, 6500106 (2014).
15. C. W. Tsao, Y. H. Cheng, and W. J. Hsueh, "Localized modes in one-dimensional symmetric Thue-Morse quasicrystals," Opt. Express **22**, 24378–24383 (2014).
16. W. J. Hsueh, C. H. Chang, and C. T. Lin, "Exciton photoluminescence in resonant quasi-periodic Thue-Morse quantum wells," Opt. Lett. **39**, 489–492 (2014).
17. J. A. Monsoriu, R. A. Depine, and E. Silvestre, "Non-Bragg band gaps in 1D metamaterial aperiodic multilayers," J. Eur. Opt. Soc. **2**, 07002 (2007).
18. H. Huang, D. Liu, H. Zhang, and X. Kong, "Electronic transport and shot noise in Thue-Morse sequence graphene superlattice," J. Appl. Phys. **113**, 043702 (2013).
19. F. Giménez, W. D. Furlan, A. Calatayud, and J. A. Monsoriu, "Multifractal zone plates," J. Opt. Soc. Am. A **27**, 1851–1855 (2010).
20. D. Pascale, *A Review of RGB Color Spaces . . . from xyY to RGB* (The BabelColor Company, 2003).
21. X. Ge, Z. Wang, K. Gao, D. Wang, Z. Z. Wu, J. Chen, Z. Pan, K. Zhang, Y. Hong, and P. Zhu, "Use of fractal zone plates for transmission X-ray microscopy," Anal. Bioanal. Chem. **404**, 1303–1309 (2012).
22. D. Keum and K.-H. Jeong, "Artificial compound eye with fractal zone plate arrays," in *Proceedings of IEEE Conference on Optical MEMS and Nanophotonics* (IEEE, 2013), pp. 31–32.
23. R. Verma, M. K. Sharma, V. Banerjee, and P. Senthilkumaran, "Robustness of Cantor diffractals," Opt. Express **21**, 7951–7956 (2013).
24. N. Gao, H. Li, X. Zhu, Y. Hua, and C. Xie, "Quasi-periodic gratings: diffraction orders accelerate along curves," Opt. Lett. **38**, 2829–2831 (2013).
25. Y. J. Liu, H. Liu, E. S. P. Leong, C. C. Chum, and J. H. Teng, "Fractal holey metal microlenses with significantly suppressed side lobes and high-order diffractions in focusing," Adv. Opt. Mater. **2**, 487–492 (2014).

1. Introduction

Zone Plates (ZPs) have found a great number of new applications in the last few years [1], especially outside of visible range of the electromagnetic spectrum, for example, in X-ray microscopy for the observation of certain nanostructures [2] and in THz optics for tomographic imaging [3]. A standard ZP consist of a series of concentric circular rings of equal area, with alternating absorbing and transmitting zones. The focusing effect is created by the constructive interference of waves passing through the transmitting zones distributed periodically along the square of the radial coordinate.

In recent years different aperiodic sequences [4] have been employed to design new types of ZPs with interesting physical properties and many potential applications. Two of them are Fractal Zone Plates [5] and Fibonacci Zone Plates [6]. The former ones are characterized by its fractal structure along the square of the radial coordinate, and produce multiple foci along the optical axis which are defined by the self-similar Fourier spectrum of the fractal pupil function. It has been demonstrated these self-similar foci produce an increase of depth of field and a reduction of the chromatic aberration under wideband illumination [7]. Since their introduction, fractal ZPs have received the attention of several research groups working on different fields, for instance, X-ray microscopy [8], optical tweezers [9], image-forming systems [10], optical tomography [11], photon sieves [12], and plasmonics [13].

Fibonacci ZPs are bifocal ZPs with their foci located at certain axial positions given by the Fibonacci numbers, being the "golden mean" the ratio of the two focal distances [6]. Although the focusing and imaging capabilities of Fibonacci lenses have been experimentally demonstrated under monochromatic illumination [14], these lenses are affected by the same limitations of conventional ZPs when broadband illumination is considered, since the twin foci are not self-similar.

In this paper we present a new family of aperiodic ZPs that combine the advantages of fractal ZPs (reduction of the chromatic aberration) and Fibonacci ZPs (bifocusing along the optical axis). The new diffractive lenses are based on the deterministic Thue–Morse sequence. This sequence has been applied in several branches of Physics, as for example in the context of photonic crystals [15], quantum wells [16], metamaterials [17] and graphene superlattices [18].

#242496 Received 8 Jun 2015; revised 13 Jul 2015; accepted 16 Jul 2015; published 22 Jul 2015

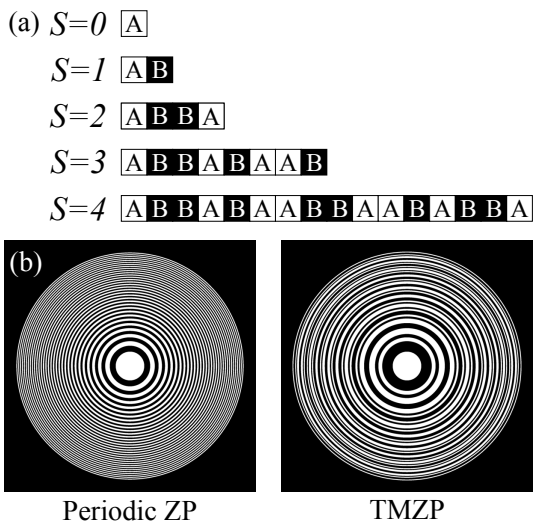

Fig. 1. a) Geometrical construction of the TM sequence up to order $S = 4$. b) TMZP of order $S = 6$ and its equivalent periodic ZP.

Here we present the first diffractive lenses contructed using this formalism. We show that a ZP designed according to the Thue–Morse sequence produces two main self-similar foci along the optical axis with extended depth of focus. Therefore, TMZPs are intrinsically bifocal lenses with low chromatic aberration. These properties are theoretically investigated and experimentally demonstrated in an image forming experiment.

2. Focusing properties

A ZP can be constructed starting from a 1D compact supported periodic function $q(\zeta)$, where $\zeta = (r/a)^2$ is the normalized square radial coordinate and a is the external radius of the outermost ring. In a binary ZP every pair of opaque (B) and transparent (A) annular zones constitutes a period, being the area of each period constant over all the ZP. In a similar way, a TMZP can be constructed by replacing the periodic function $q(\zeta)$ by the Thue–Morse sequence. This binary sequence with elements A and B is constructed defining a seed $D_0 = A$ and then, each element that follows the sequence is obtained by replacing A by AB and B by BA. Therefore, the first order is $D_1 = AB$ and the next orders are $D_2 = ABBA$, $D_3 = ABBABAAB$, $D_4 = ABBABAABBAABABBA$, and so on. Figure 1(a) shows the geometrical construction of the TM sequence up to order $S = 4$.

When designing TMZPs, each of these sequences can be used to define the transmission generating function $q(\zeta)$ with compact support on the interval $\zeta \in [0,1]$. This interval is partitioned in 2^S sub-intervals of length $d_S = 1/2^S$, and the transmitance value, $t_{S,j}$, that takes at the j-th sub-interval is associated to the value of the element $D_{S,j}$, being $t_{S,j} = 1$ when $D_{S,j}$ is "A" and $t_{S,j} = 0$ when $D_{S,j}$ is "B". Figure 1(b) shows the transmitance pupil function of a TMZP of order $S = 6$ and its equivalent periodic ZP. Note that like a conventional ZP the period of a TMZP is $p_S = 2d_S$, where the position of transparent/opaque zones have been interchanged. Therefore, the width of the zones of a TMZP and its equivalent periodic ZP are the same, so both kind of lenses can be fabricated with the same technology. In mathematical terms, the transmitance

#242496 Received 8 Jun 2015; revised 13 Jul 2015; accepted 16 Jul 2015; published 22 Jul 2015

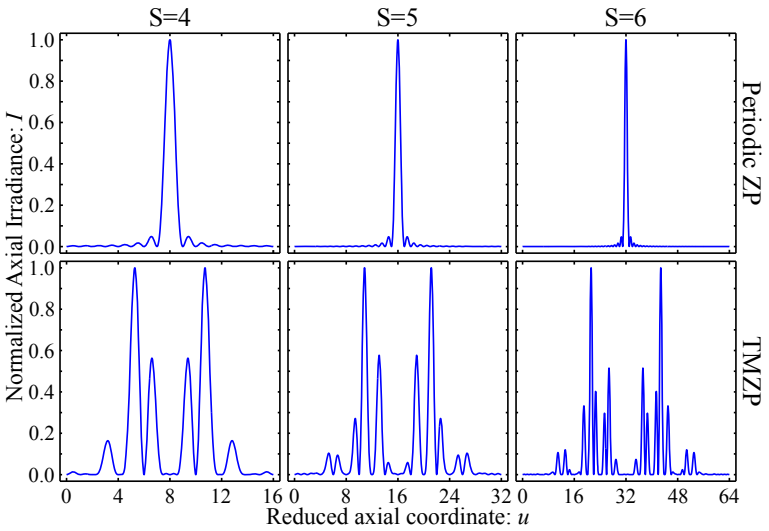

Fig. 2. Normalized axial irradiance provided by TMZPs of orders $S = 4$, 5, and 6, and their respective equivalent periodic ZPs.

function, $q(\zeta)$, for both kind of lenses can be written with the same mathematical expression

$$q(\zeta) = \sum_{j=1}^{2^S} t_{S,j} \cdot \mathrm{rect}\left[\frac{\zeta - (j-1/2)\cdot d_S}{d_S}\right]. \tag{1}$$

To evaluate the focusing properties of TMZPs we have computed the axial irradiance provided by these diffractive lenses under a monochromatic plane wave illumination, using the Fresnel approximation:

$$I(u) = 4\pi u^2 \left| \int_0^1 q(\zeta) \exp\left(-i2\pi u\zeta\right) d\zeta \right|^2, \tag{2}$$

where $u = a^2/2\lambda z$ is the reduced axial coordinate, and λ is the wavelength of the light. If we consider the pupil function of transmitance (1) in the above equation, we obtain:

$$I(u) = 4\pi^2 u^2 d_S^2 \mathrm{sinc}^2\left[d_S \cdot u\right] \left| \sum_{j=1}^{2^S} t_{S,j} e^{-i2\pi u j d_S} \right|^2. \tag{3}$$

We have computed the axial irradiance provided by TMZPs of orders $S = 4, 5,$ and 6 and their equivalent periodic ZPs for comparison. The results are shown in Fig. 2. The axial irradiance distribution, represented against the normalized variable u, shows that the reordering of transparent and opaque zones of a ZP according to the Thue–Morse sequence produces a symmetrical splitting of the first order focus achieving zero axial irradiance at the foci of the equivalent periodic ZP. This zero irradiance is due to the destructive interference produced by the fields transmited by the two conjugated parts of the lens. Therefore, TMZPs are intrinsically bifocals. Interestingly, the irradiance produced by these aperiodic lenses is characterized by a sequence of subsidiary foci around each main focus following a fractal structure. In fact, the three patterns in the lower part of Fig. 2 are selfsimilar, i.e. the irradiance distribution corresponding to a TMZP of order S is a modulated version of the irradiance distribution corresponding to the previous stage, $S-1$, magnified by a factor $\gamma = 2$.

#242496 Received 8 Jun 2015; revised 13 Jul 2015; accepted 16 Jul 2015; published 22 Jul 2015

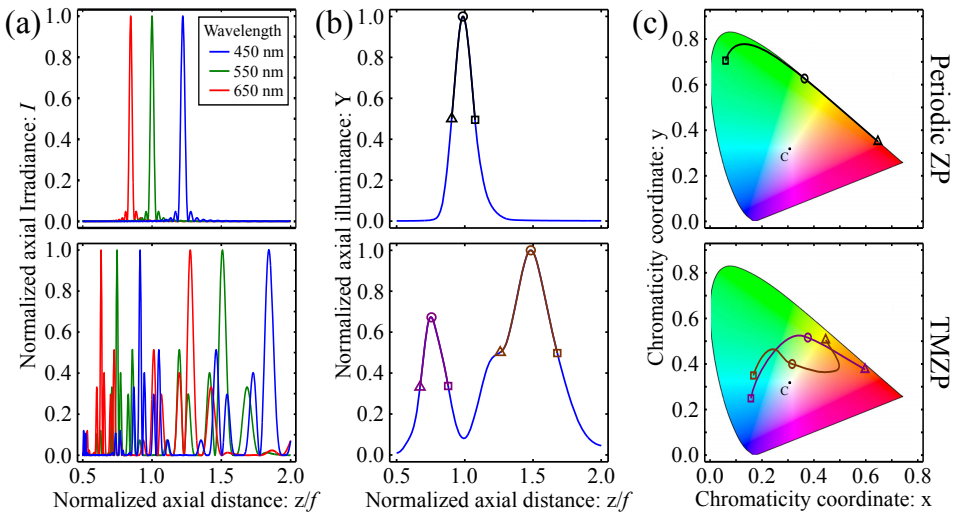

Fig. 3. a) Normalized axial irradiance for different wavelengths in the visible range, b) Normalized axial illuminance, and c) chromaticity of the different foci for the TMZP of order $S = 6$ and its equivalent periodic ZP.

In Fig. 3(a) we have represented the axial irradiances provided by a TMZP ($S = 6$) and the equivalent periodic ZP computed for three different wavelengths in the visible range ($\lambda = 450, 550$, and $650\,$nm). The axial distance, z, has been normalized to the main focal distance, $f = \frac{a^2}{\lambda 2^S}$, of the equivalent periodic ZP at $\lambda = 550\,$nm. Note that the multiple subsidiary foci around the main foci of a TMZP overlap for different wavelengths creating a pair of foci with an extended depth of focus. Therefore, a TMZP should be less sensitive to the chromatic aberration than the equivalent periodic ZP. Next, we analyze this hypothesis.

The behavior of a TMZP under broadband illumination can be evaluated, following the conventional approach [19], in terms of the tristimulus values computed along the optical axis,

$$X(z) = \int_{\lambda_1}^{\lambda_2} I(z;\lambda) S(\lambda) \tilde{x} d\lambda \,,$$
$$Y(z) = \int_{\lambda_1}^{\lambda_2} I(z;\lambda) S(\lambda) \tilde{y} d\lambda \,,$$
$$Z(z) = \int_{\lambda_1}^{\lambda_2} I(z;\lambda) S(\lambda) \tilde{z} d\lambda \,, \tag{4}$$

where $S(\lambda)$ is the spectral distribution of the source, $(\tilde{x}, \tilde{y}, \tilde{z})$ are the three sensitivity chromatic functions of the detector, and (λ_1,λ_2) represent the considered wavelength interval. In particular, in the assessment of visual systems $(\tilde{x}, \tilde{y}, \tilde{z})$ are usually the sensitivity functions of the human eye (CIE 1931) and the axial response is normally expressed in terms of the axial illuminance Y and the axial chromaticity coordinates (x, y),

$$x = \frac{X}{X+Y+Z} \,, \qquad y = \frac{Y}{X+Y+Z} \,. \tag{5}$$

To compare the performance of a TMZP under polychromatic illumination we have computed Eqs. (4) and (5) for the ZPs shown in Fig. 1. We numerically computed 41 monochromatic irradiances for equally spaced wavelengths ranging from 380 to 780 nm. The standard

#242496 Received 8 Jun 2015; revised 13 Jul 2015; accepted 16 Jul 2015; published 22 Jul 2015

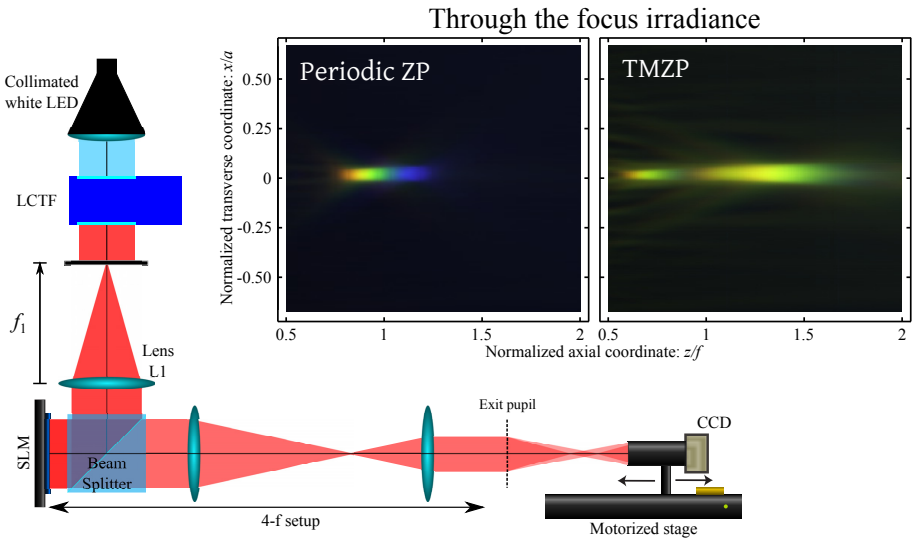

Fig. 4. Scheme of the experimental setup and the polychromatic PSFs provided by the simulated TMZP of order $S = 6$ and its equivalent periodic ZP.

illuminant C was used as a spectral distribution of the source. The illuminances computed for the TMZP of order $S = 6$ and its equivalent periodic ZP are shown in Fig. 3(b). The open circles in this figure represent the main foci of both ZPs, and the triangles and the squares represent the axial positions where the illuminance has decreased to a half of its maximum value. Figure 3(c) represents the chromatic coordinates of the axial irradiance around the main foci of the lenses. In this figure, the circles, triangles, and squares represent the chromatic coordinates at the axial points shown in Fig. 3(b). Note that the curves that reveal the chromatic content of each polichromatic focus of the TMZP are closer to the point representing the white illuminant, than the curve corresponding to the equivalent periodic ZP. Therefore the chromatic aberration of the TMZP is lower than the chromatic aberration of the equivalent binary Fresnel zone plate.

3. Experimental characterization

We have experimentally tested the polychromatic focusing properties of a TMZP developed in the presvious section. A schematic illustration of the experimental setup is shown in Fig. 4. The ZPs were implemented on a Liquid Crystal in a Silicon SLM (Holoeye PLUTO, 8-bit gray-level, pixel size $8\,\mu$m, and resolution 1920×1080 pixels), operating in amplitude mode, calibrated for different wavelengths in the visible range. The illumination system consisted of a Cold-White collimated LED (Mounted High-Power LED, CW, 1000 mA) and CRI VariSpec Liquid Crystal Tunable Filter (LCTF). This filter allows us to select a wavelength in the visible range with a bandwith of 10 nm. A pin-hole with a diameter of $150\,\mu$m was located at the focal plane of the achromatic Badal lens, L1 (focal length 160 mm). The images produced by the diffractive lenses were captured and registered with a CCD camera (8 bit gray-level, pixel pitch of $3.75\,\mu$m, and 1280×960 pixels) mounted on a translation stage (Thorlabs LTS 300; range 300 mm; precision $5\,\mu$m) along the optical axis. The images were captured at 248 axial positions for 58 wavelengths of visible light. Using Eq. (4) and transforming the tristimulus values XYZ to RGB coordinates [20], the polychromatic PSFs were obtained. Figure 4 shows the resulting polychromatic PSFs for a TMZP of order $S = 6$ and its equivalent periodic ZP with a focal distance $f = 100$ mm. As expected, the periodic ZP provides a single foci with

#242496 Received 8 Jun 2015; revised 13 Jul 2015; accepted 16 Jul 2015; published 22 Jul 2015

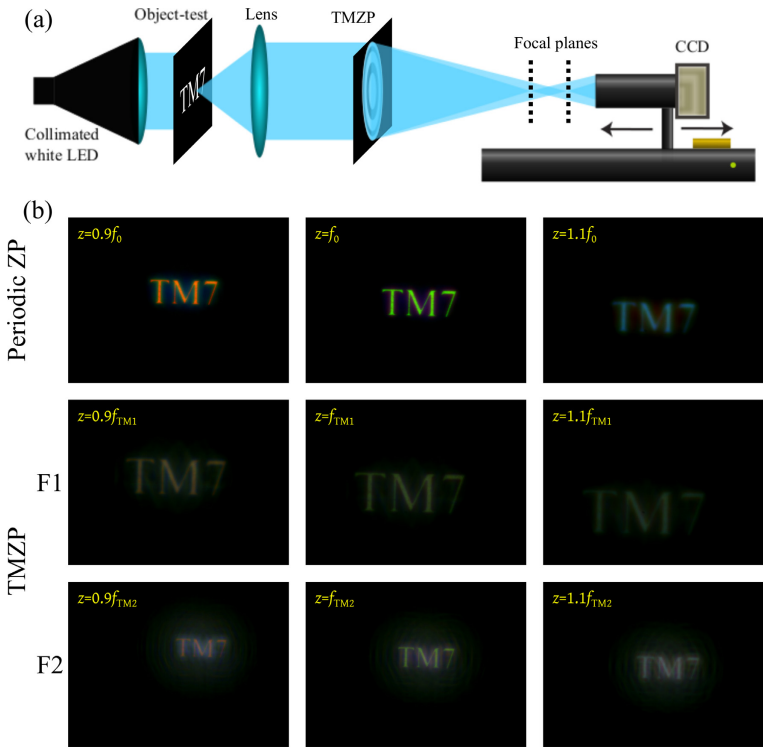

Fig. 5. Captured RGB images provided by the printed TMZP of order S_7 and its equivalent periodic ZP. The images are captured at the focal length which corresponds to every focus and around these focal planes ($\pm$10%)

high chromatic aberration, while the TMZP provides a pair of foci with enhanced focal depth and reduced chromatic aberration.

We have also tested the image forming capabilities of TMZPs under white-light illumination. In this case the binary diffractive lenses were printed on graphic films (standard polyester films) using a photoplotter with 2400 lpi resolution. We have generated a TMZP with 128 zones ($S = 7$) with $a = 3$mm (main focal distances $f_{TM1} = 188$mm and $f_{TM2} = 96$mm for a design wavelength $\lambda = 550$nm). Its equivalent periodic ZP with the same number of zones (focal distance $f_0 = 126$mm for $\lambda = 550$nm) was also constructed to compare their performances. In our experiment we considered a conventional image forming arrangement as shown in Fig. 5(a). A polychromatic light source (a cold-white LED) was employed. The object-test (binary letters "TM7") was located at the object focal plane of the achromatic lens, so the image was formed at the focal image plane of the diffractive lens. The images were captured with a CMOS Camera (EO-5012C 1/2" CMOS RGB, pixel pitch of 4.4μm). Figure 5 shows the images provided by the TMZP and by the equivalent periodic ZP at the main focal planes for the design wavelength. To obtain defocused images, the distance from the diffractive lens to the CMOS Camera was varied $\pm$10% around the focal planes. It can be seen that the TMZP provides a pair of images with a reduced chromatic aberration compared with the image provided by the periodic ZP, even at the main focal planes.

#242496 Received 8 Jun 2015; revised 13 Jul 2015; accepted 16 Jul 2015; published 22 Jul 2015

4. Conclusions

A new type of aperiodic ZPs based on the Thue-Morse sequence has been presented with interesting focusing and imaging capabilities. We have shown that a TMZP produces two self-similar foci situated symmetrically along the optical axis, one at each side of the focus of the equivalent periodic ZP of the same number of zones. As an image forming device under white light illumination, a TMZP produces a pair of images with an extended depth of field and a strong reduction in the chromatic aberration due to its bifractal focusing behavior. Therefore, TMZPs could be profitable across a broad range of applications where conventional periodic and Fractal zone plates [7] are currently applied including: spectral domain OCT [11], X-ray microscopy [8, 21], design of artificial compound eyes [22], among others [9, 23–25]. Other potential application of these aperiodic lenses will require no absortion losses and improved diffraction efficiency, as for example, bifocal intraocular or contact lens for the correction of presbyopia. To improve the diffraction efficiency of the TMZP here presented the equivalent pure phase diffractive lenses with a blazed profile are currently under study.

Acknowledgments

This work was supported by the Ministerio de Economía y Competividad (grant FIS2011-23175) and by Generalitat Valenciana (PROMETEOII/2014/072), Spain.

#242496 Received 8 Jun 2015; revised 13 Jul 2015; accepted 16 Jul 2015; published 22 Jul 2015